ACS APPLIED MATERIALS & INTERFACES

Research Article

www.acsami.org

Phage Based Green Chemistry for Gold Ion Reduction and Gold Retrieval

Magdiel I. Setyawati, Jianping Xie, and David T. Leong*

Department of Chemical and Biomolecular Engineering, National University of Singapore, 4 Engineering Drive 4, Singapore 117585, Singapore

Supporting Information

ABSTRACT: The gold mining industry has taken its toll on the environment, triggering the development of more environmentally benign processes to alleviate the waste load release. Here, we demonstrate the use of bacteriophages (phages) for biosorption and bioreduction of gold ions from aqueous solution, which potentially can be applied to remediate gold ions from gold mining waste effluent. Phage has shown a remarkably efficient sorption of gold ions with a maximum gold adsorption capacity of 571 mg gold/g dry weight phage. The product of this phage mediated process is gold nanocrystals with the size of 30−630 nm. Biosorption and bioreduction processes are mediated by the ionic and covalent interaction between gold ions and the reducing groups on the phage protein coat. The strategy offers a simple, ecofriendly and feasible option to recover of gold ions to form readily recoverable products of gold nanoparticles within 24 h.

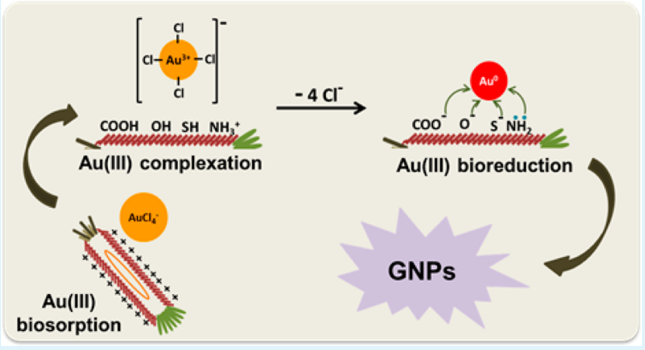

KEYWORDS: *biosorption, bioreduction, bioremediation, bacteriophage, gold nanoparticle*

INTRODUCTION

The use of gold has been woven into the fabric of human history. In modern times, gold has gone beyond its monetary functions into the realms of catalyst, nanosensors, microelectronics and nanomedicine.[1−4] Because the price of gold has exploded over recent years, the economic impetus to extract gold from ore and scrap electronics has increased. Industrial scale gold extraction involves highly toxic inorganic cyanides to bring embedded Au^0 into solution by forming a coordination complex, $Au(CN)_2^-$. The soluble form of gold is adsorbed on activated carbon and then washed, following that high temperatures and a highly alkaline medium is required for the recovery.[5] Eventually, Au^I is electrochemically reduced to Au^0.[5] The overall process is highly energy intensive, and the use of toxic chemicals at almost every step of the extraction and recovery process poses multiple threats to the environment.

Approaches to reduce the direct and indirect environmental impact of gold mining activities are underway, as evidenced by more reports highlighting benign gold mining processes. Park and Fray introduced the use of aqua-regia,[6] whereas Aydin et al. touted the use of thiourea,[7] as leaching agent substitutes, though these chemicals are still highly toxic in nature. Cyanogenic microorganisms were proposed as a safer way to extract gold from its ore.[8] In addition, various biosorption agents have been explored for more eco-friendly strategies toward supplementing part of the gold mining process.[9,10] Nevertheless, these processes still need to contend with chemical desorption in addition to electrochemical reduction.[11]

Here, we instead report a more eco-friendly methodology that may circumvent some of the gold recovery steps by utilizing bacteriophages (phages). We chose bacteriophages for several reasons. First, phages, which specifically infect bacteria, are ubiquitous and are already one of the most abundant biological entities on earth.[12] Production of the phage can be quickly and safely upscaled in mild incubation temperatures (37 °C) with basic nutrients and subsequently used directly with minimum processing, leaving an extremely low carbon footprint. Phages are chemically resistant against acidic, basic and many other organic solvents,[13−15] allowing them to withstand the harsh conditions needed to recover gold ions from the cyanide containing leachate. Filamentous bacteriophage M13 used in this study was composed of single stranded DNA packed within a proteinous cylinder coat, which contributes to 87% of the phage entity.[13,15] Thus, offering an abundance of side chain groups to facilitate the dual action of sorption and reduction of gold ions to valuable product, gold nanocrystals.[16,17] Due to their nanoscale dimensions (6.5 nm in diameter and 930 nm in length),[13] phages possess one of the highest reducing entities to mass ratio when compared to other organisms (Supporting Information Table S1).

In this study, we showed that phages were able to complex Au ions, reduce and precipitate out Au^0 in a simple one pot

Received: September 25, 2013
Accepted: December 20, 2013
Published: December 20, 2013

process in mild conditions (37 °C). Our characterization results show that gold ions were precipitated out as nanoparticles.

In addition, we showed that reduction of Au^{III} by phages resulted in biocompatible gold nanoparticles (GNPs), which can be collected easily. Collectively, our single step and one pot phage reduction-precipitation based strategy negated the commonly used process of gold ion adsorption, desorption and electrochemical reduction. This method reduces the overall chemical waste disposal burden and environmental footprint.

EXPERIMENTAL DETAILS

Materials. All chemicals were used as received without any further purification. Ultrapure water (18.2 MΩ) was used as universal solvent unless otherwise indicated. M13 bacteriophages (phages; PhD 7) were purchased from New England Biolabs. Normal human colon mucosa epithelial cells, NCM460, were provided by INCELL. Yeast extract and tryptone were acquired from Becto Dickinson. Chloroauric acid, sodium chloride (NaCl), poly ethylene glycol (PEG, MW:8000), tris base (trisaminomethane), gold single element standard for ICP and propidium iodide (PI) were purchased from Sigma Aldrich. Hydrochloric acid was obtained from Merck. Phosphate buffered saline (PBS), Dulbecco's Modified Eagle Medium (DMEM) and a penicillin/streptomycin solution were purchased from PAA. Fetal bovine serum (FBS) was supplied by ThermoScientific.

Methods. *Gold Nanoparticle (GNP) Formation.* GNPs were produced in a one pot manner whereby chloroauric acid was added to phages at final concentration 670 μM and 10^9 PFU/mL, respectively. The mixture then was shaken in either ultrapure water or PBS at 37 °C, 200 rpm for 24 h in dark conditions. The produced GNPs were collected by centrifugation (21,000 × g, 30 min), washed thrice with ultrapure water and stored at 4 °C in ultrapure water until further use.

GNP Characterization. GNPs were resuspended in methanol (to give a final concentration of 20 μg/mL) and were sonicated for 1 min to facilitate nanoparticle dispersion. Following that, the samples were dropped on carbon coated copper grids, dried at room temperature and were visualized with transmission electron microscopy (TEM; JEM-2100F, JEOL). Nanoparticle particle sizes were determined by measuring 100 randomly selected nanoparticles from TEM micrographs with ImageJ (http://rsbweb.nih.gov/ij/). Nanosphere sizes were determined from their diameters, while nanoplate sizes were represented by the length of their longest edge. Data reported are mean ± standard deviation (SD).

The hydrodynamic size and zeta potential of the produced GNPs (as synthesized) were measured with dynamic light scattering (DLS; Malvern). Measurement was done in triplicates, and the mean ± standard deviation (SD) is reported.

For the detection of gold, the produced GNPs were freeze-dried and then were mounted on the holder. Thereafter, the samples were sputtered with platinum and scanned with analytical scanning emission microscopy (SEM; JSM 5600LV, JEOL) coupled with energy dispersive X-ray spectroscopy (EDX; Inca x-act, Oxford Instruments).

To decipher the elemental composition of the sample, produced GNPs were dropped onto glass slides and left to dry overnight at 60 °C. The samples then were subjected to X-ray photoelectron spectroscopy (XPS; AXIS HIS, Kratos Analytical). Spectra were calibrated by assuming a C 1s peak at 284.5 eV as the internal standard. Deconvolution of XPS spectra was done by utilizing XPSPEAK4.1 (http://www.uksaf.org/software.html).

The absorption spectrum of GNPs was assessed with light absorbance scanning with a microplate reader (Epoch, Biotek) within a wavelength range of 400−900 nm.

Gold Recovery Determination. GNPs were produced, collected and washed thrice with ultrapure water. Thereafter, the GNPs were dissolved and the gold recovery was calculated with the help of inductive coupled plasma mass spectrometry (ICP-MS; Agilent 7500, Agilent Technologies). The amount of produced GNPs was determined using gold standard solution (TraceCERT, Sigma-Aldrich). Sorption capacity of bacteriophages was determined using the following equation:

$$\text{sorption capacity} = \frac{\text{GNP amount (mg)}}{\text{phage dry weight (g)}}$$

with 1 PFU yields 2.19×10^{-13} mg of dry weight phage pellet.[18]

Gold recovery % was calculated based on the following equation:

$$\text{recovery (\%)} = \frac{\text{GNP amount (mg)}}{\text{initial } Au^{III} \text{ amount (mg)}} \times 100\%$$

The gold recovery % and sorption capacity determination were done in triplicate, and the mean ± standard deviation (SD) data are reported.

Cell Viability Measurement. NCM460 cells were plated at 3×10^5 cells/cm^2 cell density and allowed to attach overnight. Thereafter, the cells were exposed to GNP samples (50, 250, 500 and 1000 μM) in addition to an equivalent concentration of chloroauric acid for 24 h. Complete cell culture medium was used as vehicle control. Following the exposure, all cell populations were collected and was washed twice with PBS. The cells then were stained with PI for 5 min in the dark and introduced to Tali image based cytometer (Life Technologies) for cell viability analysis. The cytotoxicity study was done in triplicate, and each viability analysis was done with a minimum of 1000 events. Data are mean ± standard deviation (SD). A statistical comparison was done with paired sample Student's *t*-test and the significance level was ascertained when $p < 0.05$.

RESULTS AND DISCUSSION

Proof of Concept of Using Phages to Reduce Gold(III) Ions. We hypothesized that the humble bacteriophage, which consists mainly of protein, could reduce gold ions. To test that hypothesis, we exposed phages to chloroauric acid solution (670 μM) prepared in two different solvents, ultrapure H_2O and phosphate buffered saline (PBS) as pH influences binding site dissociation states in addition to the hydrolysis and complexation of gold ions.[19] Phages added to gold ions resulted in a color change from yellow to deep purple (H_2O, final pH = 3.7) or to pink (PBS, final pH = 6.8). Control experiments comprising solely of phages stayed colorless, whereas the control group containing only chloroauric acid retained their yellow color. Phages exposed to chloroaurate ions (Figure 1b) showed a maximum absorbance at approximately 530 and 550 nm for reduction in PBS and H_2O, respectively. This absorption peak is attributed to GNPs' surface plasmon resonance (SPR) and was not observed in the control experiments. The maximum UV−vis absorption observed is close to that for GNPs prepared by other chemical and biological reduction techniques.[20−23]

Most importantly, we demonstrated this one pot manner of biosorption and bioreduction by phages could be done even with very dilute gold ion concentration, as evidenced by the GNP UV−vis absorption spectra (Figure 1c). Our result showed that phages could be used to reduce chloroaurate ions with concentration as low as 84 μM (~16 mg/L) in an ultrapure water reaction mixture. This result is encouraging as it enables us to overcome the traditional gold recovery limitation, which only allows recovery of gold ions higher than 100 mg/L[24] and removes trace amounts of gold in the waste effluent.

Additionally, we found that pH plays an important role to control gold ions sorption and the general gold recovery strategy. We found that by employing phages at low pH reduction condition (H_2O, pH = 3.7), we could recover back approximately 571 ± 18.6 mg gold/g of phage dry weight with an efficiency as high as 95.7 ± 3.1% . However, when neutral

dx.doi.org/10.1021/am404193j | ACS Appl. Mater. Interfaces 2014, 6, 910−917

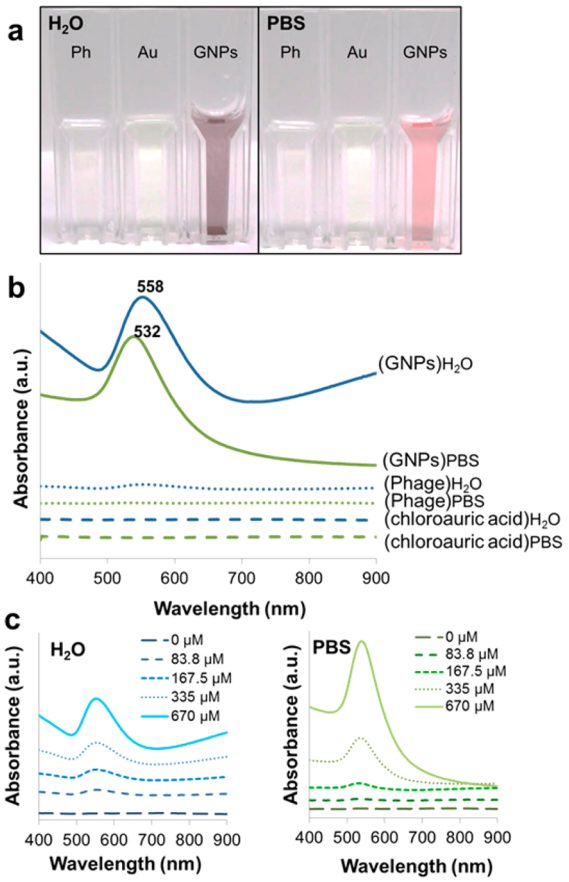

Figure 1. Bacteriophage treatment reduces gold ions into colloidal gold. (a) Mixing bacteriophage (Ph) and chloroauric acid (Au) resulted in colloidal gold (GNPs) observable via distinctive color change. (b) UV−vis absorption spectra shows characteristic peaks of colloidal gold in ultrapure water ((GNPs)H_2O) and in PBS ((GNPs)PBS). (c) Absorbance spectra showcased the capability of phage (10^9 PFU/mL) to reduce different starting concentrations of gold ions following 24 h exposure at 37 °C.

pH (PBS, pH = 6.8) was employed, the phage sorption capacity and gold recovery decreased nearly 2-fold to 306 ± 9.9 mg gold/g of phage dry weight and 51.3 ± 1.7%, respectively. It has been previously suggested that protein with its amino, sulfhydryl and carboxylic group could mediate the sorption and reduction of metal ions.[25] As pH strongly influences not only binding site dissociation but also the gold chemistry state, e.g., hydrolysis and redox state,[26] this fall in sorption capacity and gold recovery was caused by reduced binding between the phage surface and gold ions.[27] At a lower pH (pH 3.7), the pVIII protein subunit that makes up the body of the phage may become highly protonated (phage isoelectric point = 4.4).[28] On the other hand, Au^{III} exists as neutral complexes $[HAuCl_4]$ or slightly deprotonated $[AuCl_4]^-$. In neutral pH (pH 6.8), the phage carries a net negative charge while $[AuCl_4]^-$ and $[AuCl_3(OH)]^-$ complexes become the dominant form of Au^{III} species. Hence, chloroaurate ions biosorption to the positively charged and very high surface area presented on the phage body via electrostatic attraction and ion pairing is greatly promoted at lower pH and decrease as the pH increases. The governance of ionic interaction is observed for the case of gold(III) ions adsorption by *Pseudomonas maltophilia* cells, where optimum adsorption was achieved at pH 2−3 and only marginal Au^{III} adsorption at pH above 6.[27] Similarly, Ishikawa et al. reported maximum adsorption of Au^{III} on an eggshell membrane at pH 3 and no observable adsorption of Au^{III} at pH 7.[29]

Nevertheless, we reckon that ionic interaction is not the only mechanism that governs the gold ion adsorption onto the protein coat of the phage. If we take the ionic interaction as the only mode of interaction between phage protein and gold ions, then as the microenvironment of the reaction system becomes unfavorable for ionic interaction, we would expect that no gold ions get adsorbed on the phage protein coat and, in turn, no GNPs could be formed, as what has been previously described by Tsurata and Ishikawa et al.[27,29] However, there is still an appreciable amount of gold ions adsorbed onto the phage in a neutral pH system (51% recovery of gold ions), suggesting the interaction between gold(III) with phage protein coat may be covalent in nature.[30,31]

Arguably, most bioremediation strategies allow recovery of dilute gold ions with a high degree of success. Fujiwara et al. showed that 10−400 mg/L of Au^{III} could be recovered using lysine modified cross-linked chitosan resin with 100% efficiency,[32] whereas Ji et al. demonstrated a 95% recovery of 10−630 mg/L of Au^{III} with *Bacillus subtilis*.[26] Nevertheless, the use of nanodimensional phages in this study allows us to introduce the larger surface area for gold ion biosorption, resulting high biosorption and reducing capacity (Supporting Information Table S1).

Bacteriophage shows one of the highest sorption capacities almost comparable to eggshell membrane and significantly higher than synthetic materials, including the traditional adsorbents for gold remediation, i.e. activated carbon (Table 1).

Table 1. Maximum Sorption Capacity of Various Adsorbents for Au^{III} Remediation

adsorbents	sorption capacity (mg/g)	recovery (%)	ref.
organisms			
bacteriophage (M13)	571	95.7	this study
Bacillus subtilis	355	95	26
Cladosporium cladosporioides	100	80	33
biomaterials			
hen eggshell membrane	618	98	29
lysine modified cross-linked chitosan resin	70.34	100	32
synthetic materials			
activated carbon (Norit GF-40)	196	100	34
Amberlite XAD-7HP	58.8	92.3	35

Characterizations of the Bioreduced GNPs. Understanding physical, chemical and biological aspects of the product from this phage mediated bioremediation is highly important, as it allows us to reassess the feasibility and to look for any limitation to the suggested strategy. Hence, we followed-up the phage bioreduction process with characterization of bioreduced GNPs. We found that UV−vis absorption maxima generated by the reduction process in H_2O and in PBS were not identical. A distinct blue shift in addition to the narrowing of the peak could be observed when PBS was used to maintain the reduction process' environment pH (Figure 1b). We reckoned the difference in UV−vis spectra profiles between the two tested reducing conditions was caused by the different GNP morphologies being formed in the reaction mixture. To validate our initial deduction, we viewed the reduction product

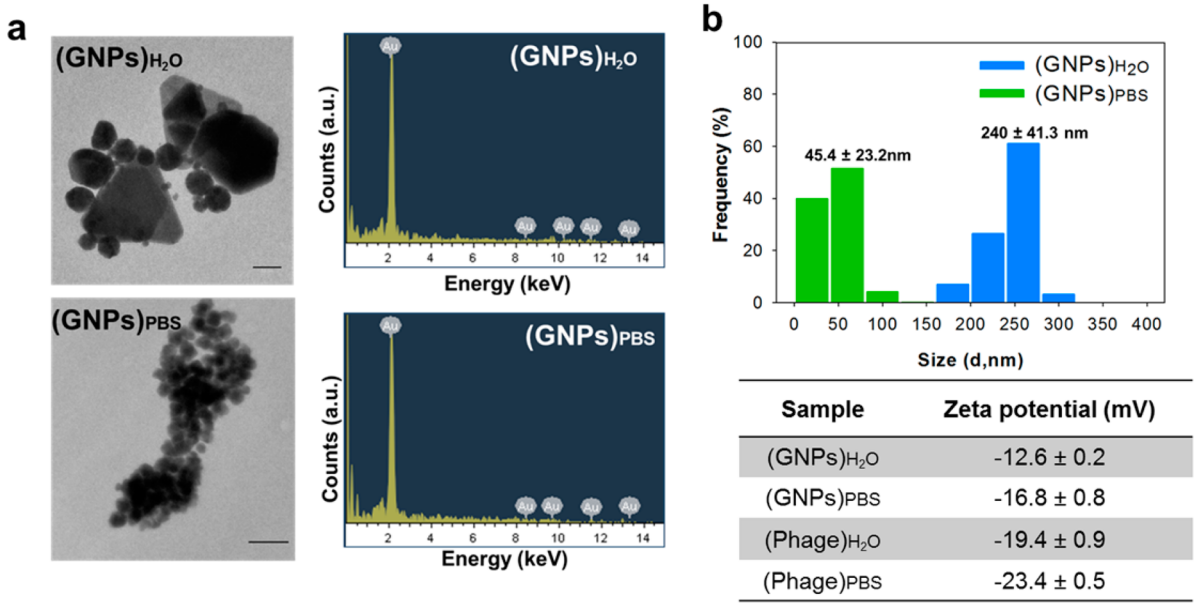

Sample	Zeta potential (mV)
$(GNPs)_{H_2O}$	-12.6 ± 0.2
$(GNPs)_{PBS}$	-16.8 ± 0.8
$(Phage)_{H_2O}$	-19.4 ± 0.9
$(Phage)_{PBS}$	-23.4 ± 0.5

Figure 2. Characterizations of GNPs. (a) TEM images showed the shape and size distributions of GNPs in ultrapure H_2O and PBS. Scale bar = 50 nm. EDX detected the presence of gold element on the produced nanoparticles. (b) Hydrodynamic size and zeta potential of GNPs determined from Dynamic Light Scattering (DLS). Data are mean ± SD, n = 3.

with transmission electron microscopy (TEM) and further analyzed with energy dispersive X-ray (EDX). Representative TEM micrographs and EDX data (Figure 2a) revealed that a diversity of shapes and sizes of GNPs were formed under the two reducing conditions. Reduction reaction in H_2O yielded in a mixture of triangle nanoplates and spherical nanoparticles. Statistical analysis indicates that nearly 40% of the total population consists of triangular nanoplates with a length range of 30−630 nm (average length = 188.75 ± 107.3 nm). The rest of the population consists of nanospheres with an average size of 37.9 ± 12.7 nm, whereas the reduction process in PBS yielded more discrete spherical nanoparticles with an average size of 15.1 ± 4.4 nm. These results indicate that pH plays an important role on the reduction process and morphology control of the produced GNPs. As described previously, the amine groups in protein coat are protonated at lower pH, whereas chloroaurate ions are present in the form of negatively charged $[AuCl_4]^-$. Though this condition will promote the chloroaurate ions attraction to the binding site of phage body protein pVIII,[36] the same condition does not favor the reduction process, which was substantiated by the low reaction rate and reduction power.[20] As a result, the slower reduction process could not keep pace with the faster adsorption of gold ions onto phage proteins, resulting in the formation of anisotropic nanoplates.[37] With the increase of pH, the adsorption rate becomes more dampened to a level that matches the reducing reaction rate, resulting in gold ions being reduced as soon as they are adsorbed on the phage and, in contrast, promoted the formation of isotropic spherical nanoparticles.

Further analysis with dynamic light scattering (DLS) showed the hydrodynamic size of GNPs to be bigger than the sizes acquired from the TEM (Figure 2b). This could be attributed to not only solvation between GNPs and the solvent but also to the presence of phage protein on the surface of the bioreduced GNPs, forming a shell of protective coat. In addition, this hydrodynamic data suggested that the produced GNPs might be forming aggregates, which actually favors easy recovery. Phage initial ζ-potentials were registered at −19.4 ± 0.9 and −23.4 ± 0.5 in aqueous and PBS medium, respectively. Upon Au^{III} adsorption and reduction processes, the produced GNPs' net ζ-potentials were registered at −12.6 and −16.8 mV for reduction at low pH (H_2O) and neutral pH (PBS), respectively. The negative charge registered for our GNPs indicates the presence of biomolecules on the surface of the nanoparticles and imparting its negative charge. Our reading is close to what has been reported in the bovine serum albumin (BSA) capped GNPs, which was found to be negatively charged (−20 mV at pH = 5).[38] Slight differences might be caused by the fact that phage protein compromised of different amino acids compositions from those in BSA.

To attempt to further elucidate how the phage protein could be used to reduce the gold ions, we conducted X-ray photoelectron spectroscopy (XPS) analysis. Our wide scanning XPS spectra (Figure 3a) identified spectra specific to Au core in addition to those specific to organic compounds, e.g. C 1s, N 1s and O 1s. High resolution scanning of Au 4f (Figure 3b) revealed doublet signal peaks of $4f_{7/2}$ and $4f_{5/2}$, which correspond to the presence of Au^0.[25,39,40] These gold specific spectra could only be detected on the bioreduced GNPs and not on the control experiment comprised of phages. Au 4f core scanning revealed that the doublet peaks from both reduction systems did not coincide perfectly, suggesting that more than one species of gold is present on the samples. Deconvolution of the Au $4f_{7/2}$ peak (Supporting Information Figure S1) showed the presence of two other species of gold on the GNPs, Au^0 and Au^I. Bioreduction conducted in aqueous medium resulted in peaks at binding energies of 84.1 and 84.9 eV specific to Au^0 and Au^I, respectively.[25,39,40] Similarly, phage mediated reduction in PBS resulted in the peaks to appear at binding energies of 83.8 and 84.3 eV assigned to Au^0 and Au^I, respectively.[39,40] We could not detect the presence of the Au^{III} species, which indicates that all of Au^{III} was reduced to Au^I and Au^0. According to Isab and Sadler, Au^{III} is initially reduced to Au^I and followed by a much slower reduction to Au^0.[41] The presence of the Au^I species signifies that a longer phage

dx.doi.org/10.1021/am404193j | ACS Appl. Mater. Interfaces 2014, 6, 910−917

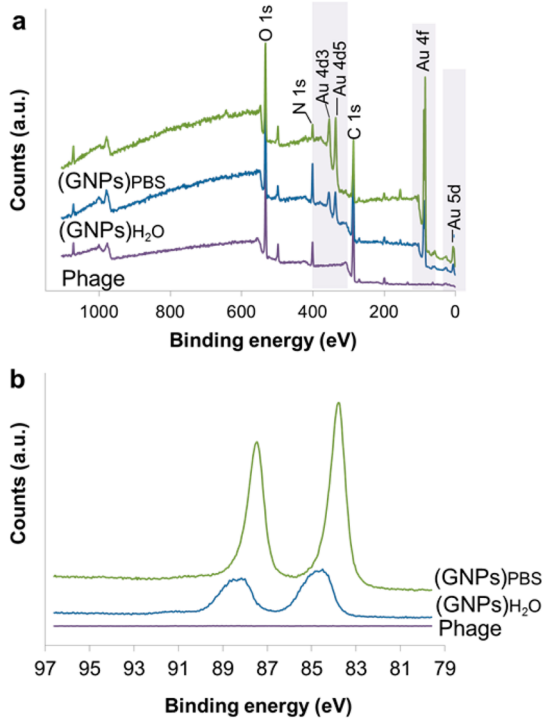

Figure 3. Elemental analysis of bioreduced GNPs. (a) X-ray photoelectron spectroscopy (XPS) wide scan survey shows the gold characteristic peaks in addition to peaks specific to organic compounds. (b) XPS Au 4f high scan spectra of phage in addition to gold NPs produced in ultrapure water ((GNPs)H_2O) and PBS ((GNPs) PBS).

mediated bioreduction process is necessary to fully reduce Au^{III} to Au^0, as demonstrated by Das et al., whereby the concentration of the Au^I species decreases while the concentration of the Au^0 species increases following an increase in bioreduction time with *Rhyzopus oryzae*.[31] In addition, XPS analysis allowed us to roughly estimate the conversion of Au^{III} to Au^0. We found that phage mediated reaction done in PBS yielded close to a 2-fold increase in the conversion percentage when compared to the reduction process conducted in H_2O. A higher conversion percentage in the PBS system is in agreement with our initial thought whereby neutral pH could offer a faster reduction rate and a higher reduction power of Au^{III} to Au^0. Beside the slower reduction rate in the H_2O system, the Au^I species, which was present on the surface of the GNPs, could potentially block the Au^0 signal and further reduce the amount of Au^0 species getting detected. As a result, the Au^{III} to Au^0 conversion in H_2O gets diminished further from its true value.

The presence of peaks specific for an organic material such as O 1s, C 1s, and N 1s on GNP samples can be associated to biomolecules on the surface of the produced GNPs. Deconvolution of C 1s spectra (Supporting Information Figure S1, Table S2) yielded five species that can be attributed to phage proteins on the GNP surface. The peak at 284.5 eV could be assigned to C—C and C—H, while carbon bound to nitrogen and hydroxyl group (C—OH) could be detected at 285.0 and 285.6 eV, respectively. The peak at 286.4 eV represents the presence of carbonyl groups, whereas the peak at 288.0 eV corresponds to a carboxylate functional group and carbon in the amide group from the protein molecules. Correspondingly, O 1s spectra, when resolved (Supporting Information Figure S1, Table S2), resulted in three distinct peaks. Carboxylic groups could be detected via C═O and C—OH signal which were located at binding energy of 532.2 and 533.0 eV, respectively. Signal at 531.3 eV could be attributed to the carbonyl group bounded to the nitrogen atom of asparagine and glutamine amino acid in the phage protein.

In addition, through N 1s scanning, we could detect the phage N 1s core level at 399.7 and 401.0 eV (Supporting Information Figure S1, Table S2), assigned to the unprotonated amine/amide species and protonated amine species, respectively,[42] which are present in phage protein. Following the bioreduction process, we could detect only unprotonated species of amine/amide groups for the reduction carried out in both water and PBS medium, which appeared at slightly higher binding energies of 399.9 and 400.1 eV, respectively. Shifting of binding energies, which correspond to carboxylate and amine groups following metal ion exposure, have been identified as an indicator of interaction between these functional groups with the metal nanoparticles.[22,31] Moreover, the relative content change in N 1s core suggested that the phage's reducing capability is determined by the amino group in the protein coat. It has been suggested that the amine group of the amino acid is responsible for facilitating reduction of the gold ion. The amine group donates its electron to the gold ion, which subsequently results in the formation of GNPs.[43]

Our findings thus far suggest that phage could facilitate gold ion recovery through the following two steps: (i) binding of gold ions to proteins on phage wall through ionic and covalent interactions followed by (ii) reduction, which was facilitated by functional groups of the protein molecules (Scheme 1). Arguably, our result does not encompass the complete library of functional groups, which could mediate the gold recovery

Scheme 1. Illustration of Phage Mediated Gold Ion Biosorption and Bioreduction Process[a]

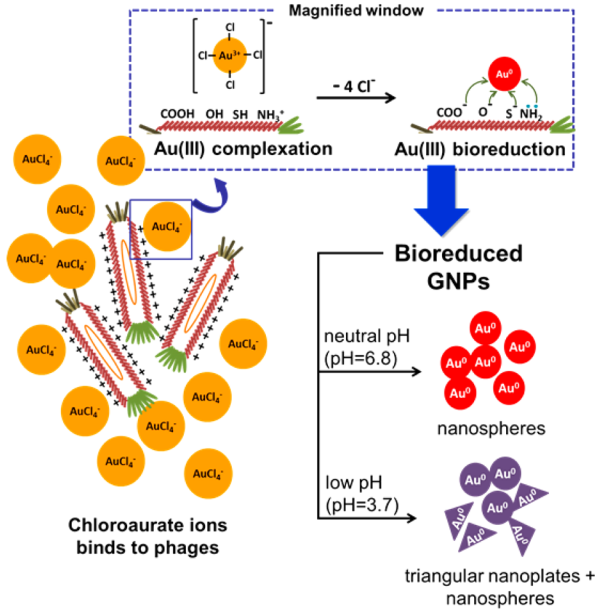

[a]Gold biosorption to phage wall is mediated by the ionic interaction between negatively charged chloroaurate ions and positively charged moieties of the phage protein coat. Following that, the gold ions were complexed and bioreduced to produce GNPs. Depending on the pH of the reduction reaction, nanospheres, GNPs or a mixture of triangle nanoplates and nanospheres could be produced.

dx.doi.org/10.1021/am404193j | ACS Appl. Mater. Interfaces 2014, 6, 910−917

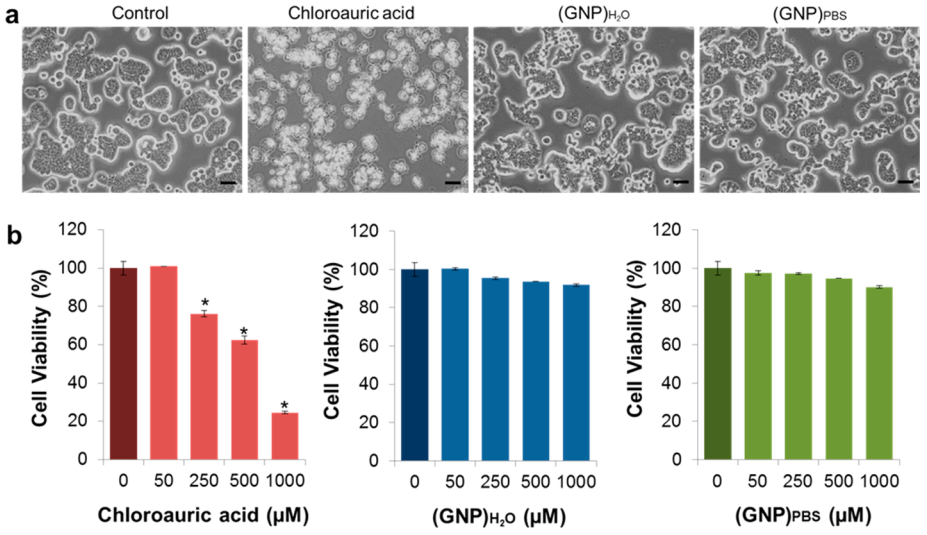

Figure 4. Gold remediation by phages reduce harmful chloroauric acid to harmless GNPs. (a) phase contrast images show that the gold ions exerted a cytotoxic effect on NCM460 cells, as evidenced by the cells' morphological changes following exposure of 1000 μM chloroauric acid for 24 h. (b) Cytotoxicity of chloroauric acid was ascertained by cell viability results, as evidenced by dose dependent toxicity of NCM460 cells following 24 h exposure of chloroauric acid in various concentrations. Data are mean ± SD, $n = 3$, Student's t-test, $p < 0.05$, an asterisk indicates significance against the untreated control.

process. Nevertheless, we have identified several functional groups including phenolic, carboxylic, carbonyl and amine groups to be involved in the process. Our findings are consistent with previous reports, which describe the role of amino acids or complex proteins to form GNPs.[22,25,31,43]

Gold Reduction Phage Strategy for a More Sustainable Gold Production Process. Though understanding the physical and chemical aspects of the process and the produced GNPs is important, the picture is not yet complete without any biological characterization of the produced GNPs. Gold remediation is necessary not only for the purpose of recovering the precious gold (from even dilute solutions) for commercial gain but also necessitated by the potential harm of gold ions when released irresponsibly to the environment. One of our aims was to use this phage mediated reduction of gold ions for remediation of gold ions from the waste effluent. Hence, this biological characterization is needed to verify the suitability of this strategy in alleviating the toxic waste load released to the environment. Using normal human colon cell lines as a cell model, we found that these cells were sensitive to gold ions. We observed the cells lost cellular contact with their neighboring cells upon exposure to 1000 μM of gold ions (24 h). In addition, the cells shrunk and finally detached from the plate, signifying cell death, as can be observed in Figure 4a. We further confirmed gold ion toxicity by measuring cell viability. Our cell viability data also corroborated with our microscopic observations; whereby cells exposed to gold ions showed a dose dependent cell death. We observed a nearly 70% reduction in cell viability when compared to an untreated control with 24 h exposure to gold ions (Figure 4b). Initially, we suspected that the acidity in the chloroauric acid solution was the reason for significant cell death. However, we measured the pH of the cell culture media with 1000 μM chloroauric acid solution, and pH remained at the original cell culture medium of 7.4, indicating that acidity in the final preparation was not the reason for the observed toxicity. This also suggested that the toxicity that we observed was caused by gold ions. Similarly, studies have reported that metallic ions, including gold ions, are highly reactive and posed some toxicity to organisms.[44−47] Au^{III} ions inhibited microbial metabolism[48] and induced photomutagenicity.[49] Au^{III} also induced toxic histamine release from human basophils cells.[50]

The next issue to be addressed is whether cellular toxicity of gold ions can be diminished when gold is bioreduced by phages. In stark contrast to the gold ion treated group, after exposing both types of GNPs produced by phages, we observed no obvious cellular morphological changes and the cells looked identical to the nontreated control. Our viability data further confirmed the biocompatibility of the bioremediated GNPs. Overall, we detected no significant changes on cell viability upon exposure of GNPs for 24 h. This finding is also in line with the reports demonstrating general GNP biocompatibility.[51,52]

Collectively, phages have been demonstrated to be able to mediate biosorption of reactive gold ions and to facilitate their reduction to harmless GNPs. We have shown through a simple one pot manner at room temperature using cheap and highly renewable and harmless phages that gold ions could be reduced and recovered. Moreover, due to their small dimensions, phages offer a much higher adsorption capacity when compared to most adsorbents, allowing a smaller number of phages to be actually introduced to recover gold from the effluent. The ease of propagating the phages allows the bioreduction process to occur incessantly and to avoid the unnecessary effect of seasonal variations and husbandry product availability. There is no need to process the phages as it can be used as it is versus other biomaterials mediated methods where the active ingredients need to be processed before use. Additionally, our strategy allows the gold reduction to take place in situ and in the bulk environment, independent of cell uptake and/or cell metabolism to express necessary enzymes for the reduction. The subsequent downstream collection process is simplified tremendously as compared to the industrial method involving gold desorption from the inorganic adsorbents and high carbon footprint electrochemical reduction could be avoided. The phages could bioreduce a very dilute concentration of gold ions suggestive that this strategy can be used as an environmental remediation tool for very dilute gold contaminants (but still

poses significant harm) in water bodies. This eco-friendly strategy might be able to remediate other type of heavy metal contaminants, e.g. mercury, platinum, palladium and silver. Lastly, phages already exist in nature and are harmless to humans as they only infect bacteria. Admittedly, there are few aspects that need to be addressed before this strategy could be realized in the industrial setting. Improving biosorption capacity as well increasing the reducing potential of the phage for an optimal recovery process is one of them. This could be approached by tailoring the genomic information of the phage, thus allowing the phage protein coat to display functional groups with a higher reducing capability. At the same time, genomic tailoring allows the phage to be more discriminative toward gold ions, resulting in highly selective retrieval. Another problem that needs to be tackled is the scalability of this strategy. As the present investigation was done on a lab scale, the ability of this strategy to perform on a much larger scale still needs to be further studied.

CONCLUSION

Herein, we demonstrated one pot biosorption and bioreduction of gold ions using phage. We showed that we able to recover a large percentage of gold ions introduced with an impressively high gold sorption capacity of 571 mg/g dry weight phage, allowing fewer phages to be used for the sorption process when compared to other adsorbents. The strategy is important as it provides a simple, eco-friendly feasible option to recover gold ions, allowing the omission of downstream steps and lessening the total chemical waste load. This phage mediated bioreduction is expected to be applicable for other type of heavy metal contaminants remediation.

ASSOCIATED CONTENT

Supporting Information

Meta analysis of bacteriophage entities to mass ratio. Phage amplifications, cell culture and GNP samples preparation for toxicity assay (Experimental details). Additional data consisting of XPS spectra deconvolution (Figure S1) and XPS peaks assignment and atomic composition of samples' surface (Table S2). This material is available free of charge via the Internet at http://pubs.acs.org.

AUTHOR INFORMATION

Corresponding Author

*D. T. Leong. Phone: 65-6516 7262. Fax: 65-6779 1936. E-mail: cheltwd@nus.edu.sg.

Author Contributions

M.I.S designed and carried out the experiments, performed the analysis, and wrote the paper. X.J. wrote the paper. D.T.L conceived the hypotheses and concepts and wrote the paper. All authors read and approved the final manuscript.

Notes

The authors declare no competing financial interest.

ACKNOWLEDGMENTS

We thank Mr. Luo Zhentao for his technical assistance with TEM. This study was funded by Ministry of Education Academic, Singapore (R-279-000-350-112 to D.T.L). M.I.S is a recipient of the research scholarship from National University of Singapore.

ABBREVIATIONS

DLS, dynamic light scattering
DMEM, Dulbecco's Modified Eagle Medium
EDX, energy dispersive X-ray spectroscopy
FBS, fetal bovine serum
GNPs, gold nanoparticles
PBS, phosphate buffered saline
PEG, poly ethylene glycol
PFU, plague forming unit
PI, propidium iodide
SEM, scanning electron microscope
TBS, tris buffered saline
TEM, transmission electron microscopy
Tris, trisaminomethane
XPS, X-ray photoelectron spectroscopy

REFERENCES

(1) Dasary, S. S. R.; Senapati, D.; Singh, A. K.; Anjaneyulu, Y.; Yu, H.; Ray, P. C. *ACS Appl. Mater. Interfaces* **2010**, *2*, 3455−3460.
(2) Niikura, K.; Iyo, N.; Matsuo, Y.; Mitomo, H.; Ijiro, K. *ACS Appl. Mater. Interfaces* **2013**, *5*, 3900−3907.
(3) Beqa, L.; Fan, Z.; Singh, A. K.; Senapati, D.; Ray, P. C. *ACS Appl. Mater. Interfaces* **2011**, *3*, 3316−3324.
(4) Yang, H.; Nagai, K.; Abe, T.; Homma, H.; Norimatsu, T.; Ramaraj, R. *ACS Appl. Mater. Interfaces* **2009**, *1*, 1860−1864.
(5) Bhappu, R. B. In *Gold - Advances in Precious Metal Recovery*, 1st ed.; Arbiter, N., Han, K. N., Eds.; Gordon and Breach Science Publishers: New York, 1990, pp 67−79.
(6) Park, Y. J.; Fray, D. J. *J. Hazard Mater.* **2009**, *164*, 1152−1158.
(7) Aydin, A.; Kaki, E.; Aydin, A. A. *Sep. Sci. Technol. (Philadelphia, PA, U. S.)* **2001**, *36*, 3239−3251.
(8) Shin, D.; Jeong, J.; Lee, S.; Pandey, B. D.; Lee, J.-c. *Miner. Eng.* **2013**, *48*, 20−24.
(9) Mack, C.; Wilhelmi, B.; Duncan, J. R.; Burgess, J. E. *Biotechnol. Adv.* **2007**, *25*, 264−271.
(10) Sathish Kumar, K.; Amutha, R.; Palaniappan, A.; Sheela, B. *ACS Appl. Mater. Interfaces* **2011**, *3*, 1418−1425.
(11) Syed, S. *Hydrometallurgy* **2012**, *115*, 30−51.
(12) Bergh, O.; Borsheim, K. Y.; Bratbak, G.; Heldal, M. *Nature* **1989**, *340*, 467−468.
(13) Webster, R. In *Phage Display, a Laboratory Manual*, 1st ed.; Barbas, C. F., III; Burton, D. R.; Scott, J. K.; Silverman, G. J., Eds.; Cold Spring Harbor Lab. Press: New York, 2001, pp 1.1−1.37.
(14) Jończyk, E.; Kłak, M.; Międzybrodzki, R.; Górski, A. *Folia Microbiol.* **2011**, *56*, 191−200.
(15) Petrenko, V. A.; Vodyanoy, V. J. *J. Microbiol. Methods* **2003**, *53*, 253−262.
(16) Niu, H.; Volesky, B. *J. Chem. Technol. Biotechnol.* **2000**, *75*, 436−442.
(17) Volesky, B., *Sorption and Biosorption*; BV Sorbex Inc: Montreal, 2003.
(18) Kolstad, R. A.; Bradley, S. G. *J. Bacteriol.* **1966**, *91*, 1372−1373.
(19) Fiol, N.; Villaescusa, I.; Martinez, M.; Miralles, N.; Poch, J.; Serarols, J. *(Philadelphia, PA, U. S.)* **2006**, *50*, 132−140.
(20) He, S. Y.; Guo, Z. R.; Zhang, Y.; Zhang, S.; Gu, J. W. N. *Mater. Lett.* **2007**, *61*, 3984−3987.
(21) Kwon, K.; Lee, K. Y.; Lee, Y. W.; Kim, M.; Heo, J.; Ahn, S. J.; Han, S. W. *J. Phys. Chem. C* **2007**, *111*, 1161−1165.
(22) Mukherjee, P.; Ahmad, A.; Mandal, D.; Senapati, S.; Sainkar, S. R.; Khan, M. I.; Ramani, R.; Parischa, R.; Ajayakumar, P. V.; Alam, M.; Sastry, M.; Kumar, R. *Angew. Chem., Int. Ed.* **2001**, *40*, 3585−3588.
(23) Hormozi-Nezhad, M. R.; Karami, P.; Robatjazi, H. *RSC Adv.* **2013**, *3*, 7726−7732.
(24) Nourbakhsh, M.; Sag, Y.; Ozer, D.; Aksu, Z.; Katsal, T.; Calgar, A. *Process Biochem.* **1994**, *29*, 1−5.
(25) Xie, J.; Lee, J. Y.; Wang, D. I.; Ting, Y. P. *Small* **2007**, *3*, 672−682.

(26) Ji, Y. L.; Gao, H.; Sun, J. S.; Cai, F. *Chem. Eng. J.* **2011**, *172*, 122−128.
(27) Tsuruta, T. *J. Gen. Appl. Microbiol.* **2004**, *50*, 221−228.
(28) Rong, J.; Lee, L. A.; Li, K.; Harp, B.; Mello, C. M.; Niu, Z.; Wang, Q. *Chem. Commun.* **2008**, 5185−5187.
(29) Ishikawa, S.; Suyama, K.; Arihara, K.; Itoh, M. *Bioresour. Technol.* **2002**, *81*, 201−206.
(30) Greene, B.; Hosea, M.; McPherson, R.; Henzl, M.; Alexander, M. D.; Darnall, D. W. *Environ. Sci. Technol.* **1986**, *20*, 627−632.
(31) Das, S. K.; Liang, J.; Schmidt, M.; Laffir, F.; Marsili, E. *ACS Nano* **2012**, *6*, 6165−6173.
(32) Fujiwara, K.; Ramesh, A.; Maki, T.; Hasegawa, H.; Ueda, K. *J. Hazard Mater.* **2007**, *146*, 39−50.
(33) Pethkar, A. V.; Paknikar, K. M. *J. Biotechnol.* **1998**, *63*, 121−136.
(34) Paclawski, K.; Wojnicki, M. *Arch. Metall. Mater.* **2009**, *54*, 853−860.
(35) Van Nguyen, N.; Lee, J. C.; Kim, S. K.; Jha, M. K.; Chung, K. S.; Jeong, J. *Gold Bull. (Berlin, Ger.)* **2010**, *43*, 200−208.
(36) Drummy, L. F.; Jones, S. E.; Pandey, R. B.; Farmer, B. L.; Vaia, R. A.; Naik, R. R. *ACS Appl. Mater. Interfaces* **2010**, *2*, 1492−1498.
(37) Sajanlal, P. R.; Sreeprasad, T. S.; Samal, A. K.; Pradeep, T. *Nano. Rev.* **2011**, *2*, 5883.
(38) Brewer, S. H.; Glomm, W. R.; Johnson, M. C.; Knag, M. K.; Franzen, S. *Langmuir* **2005**, *21*, 9303−9307.
(39) Xie, J. P.; Zheng, Y. G.; Ying, J. Y. *J. Am. Chem. Soc.* **2009**, *131*, 888−889.
(40) Corma, A.; Garcia, H. *Chem. Soc. Rev.* **2008**, *37*, 2096−2126.
(41) Isab, A. A.; Sadler, P. J. *Biochim. Biophys. Acta* **1977**, *492*, 322−330.
(42) Amaral, I. F.; Granja, P. L.; Barbosa, M. A. *J. Biomater. Sci., Polym. Ed.* **2005**, *16*, 1575−1593.
(43) Wangoo, N.; Bhasin, K. K.; Mehta, S. K.; Suri, C. R. *J. Colloid Interface Sci.* **2008**, *323*, 247−254.
(44) Setyawati, M. I.; Tay, C. Y.; Leong, D. T. *Biomaterials* **2013**, *34*, 10133−10142.
(45) Ng, K. W.; Khoo, S. P. K.; Heng, B. C.; Setyawati, M. I.; Tan, E. C.; Zhao, X.; Xiong, S.; Fang, W.; Leong, D. T.; Loo, J. S. C. *Biomaterials* **2011**, *32*, 8218−8225.
(46) Cho, W. S.; Duffin, R.; Howie, S. E.; Scotton, C. J.; Wallace, W. A.; Macnee, W.; Bradley, M.; Megson, I. L.; Donaldson, K. *Part. Fibre Toxicol.* **2011**, *8* (27), 1−16.
(47) Cheng, X.; Zhang, W.; Ji, Y.; Meng, J.; Guo, H.; Liu, J.; Wu, X.; Xu, H. *RSC Adv.* **2013**, *3*, 2296−2305.
(48) Johnston, C. W.; Wyatt, M. A.; Li, X.; Ibrahim, A.; Shuster, J.; Southam, G.; Magarvey, N. A. *Nat. Chem. Biol.* **2013**, *9*, 241−243.
(49) Wang, S. G.; Lawson, R.; Ray, P. C.; Yu, H. T. *Toxicol. Ind. Health* **2011**, *27*, 547−554.
(50) Schedle, A.; Samorapoompichit, P.; Fureder, W.; Rausch-Fan, X. H.; Franz, A.; Sperr, W. R.; Sperr, W.; Slavicek, R.; Simak, S.; Klepetko, W.; Ellinger, A.; Ghannadan, M.; Baghestanian, M.; Valent, P. *J. Biomed. Mater. Res.* **1998**, *39*, 560−567.
(51) Zhang, Q.; Hitchins, V. M.; Schrand, A. M.; Hussain, S. M.; Goering, P. L. *Nanotoxicology* **2011**, *5*, 284−295.
(52) Shukla, R.; Bansal, V.; Chaudhary, M.; Basu, A.; Bhonde, R. R.; Sastry, M. *Langmuir* **2005**, *21*, 10644−10654.